Steel and Composite Structures, *Vol. 21, No. 2 (2016) 343-356*
DOI: http://dx.doi.org/10.12989/scs.2016.21.2.343

Study on seismic performance of connection joint between prefabricated prestressed concrete beams and high strength reinforcement-confined concrete columns

Haotian Jiang *1, Qingning Li [1], Weishan Jiang [1] and De-Yi Zhang [2]

[1] *School of Civil Engineering, Xi'an University of Architecture and Technology, Xi'an 710055, China*
[2] *Department of Engineering Mechanics, Ontario Power Generation, Toronto, ON, M5G 1Z5, Canada*

(*Received November 11, 2015, Revised April 01, 2016, Accepted April 11, 2016*)

Abstract. As the common cast-in-place construction works fails to meet the enormous construction demand under rapid economic growth, the development of prefabricated structure instead becomes increasingly promising in China. For the prefabricated structure, its load carrying connection joint play a key role in maintaining the structural integrity. Therefore, a novel end plate bolt connecting joint between fully prefabricated pre-stressed concrete beam and high-strength reinforcement-confined concrete column was proposed. Under action of low cycle repeated horizontal loadings, comparative tests are conducted on 6 prefabricated pre-stressed intermediate joint specimens and 1 cast-in-place joint specimen to obtain the specimen failure modes, hysteresis curves, skeleton curves, ductility factor, stiffness degradation and energy dissipation capacity and other seismic indicators, and the seismic characteristics of the new-type prefabricated beam-column connecting joint are determined. The test results show that all the specimens for end plate bolt connecting joint between fully prefabricated pre-stressed concrete beam and high-strength reinforcement-confined concrete column have realized the design objectives of strong column weak beam. The hysteretic curves for specimens are good, indicating desirable ductility and energy dissipation capacity and seismic performances, and the research results provide theoretical basis and technical support for the promotion and application of prefabricated assembly frames in the earthquake zone.

Keywords: pre-stressed structure; beam-column joint; low cycle loading; shear resistance of joint; ductility factor

1. Introduction

The development of prefabricated structural system is the only way for industrialization of building (Rao and Sundaresan 2012, Hossain *et al*. 2011, Mu *et al*. 2013, Ho *et al*. 2013, Sasmal *et al*. 2011, Niroomandi *et al*. 2010, Yao 2010). In recent years, domestic and foreign scholars carried out a lot of experimental research and theoretical analysis on the seismic performance of structural systems, and achieved remarkable results (Karayannis and Sirkelis 2008, Pantelides *et al*. 2008, Lee *et al*. 2010, Zenunović and Folić 2012, Ma *et al*. 2013, Zhang *et al*. 2013, Ban 2011, Shi *et al*. 2013, Liu *et al*. 2012, Liang *et al*. 2010, Liu *et al*. 2011, Hou 2011, Xu *et al*. 2013, Jian *et al*. 2013, Zhao *et al*. 2012). The wet operations on the cast-in-place concrete girder-column joints are in

*Corresponding author, Ph.D., E-mail: 316195906@qq.com

Copyright © 2016 Techno-Press, Ltd.
http://www.techno-press.org/?journal=scs&subpage=6 ISSN: 1229-9367 (Print), 1598-6233 (Online)

relatively large quantities, and the placement of reinforcement at the joints is rather complex, thus is not conducive to construction procedures, e.g., pouring and vibration.

Compared between prefabricated structures and cast-in-place structures, the most prominent characteristic lies in the different connection methods, the frame structure form is widely used in residential building, while the joint is a key component in the beams and columns load transfer in structure. Especially under seismic action, the integrity and seismic behavior determine the failure mode and work performance of the entire structure, and therefore the studies on seismic performance of beam - column joint has great significance for understanding and knowledge of the seismic performance of the prefabricated structure.

This paper introduces the end plate bolt joint commonly used in steel structure into concrete structure, the high-strength bolts are used to connect the end plate and the steel plate stirrup on the concrete column, and apply the pre-stress force. The beam longitudinal plain rebar is connected to the end plate in the form of the button-head welding, and the pre-stressing bars are anchored with nuts, thereby forming a new form of prefabricated joint. This test studied and analyzed the seismic performance and force mechanism for the end plate bolt connecting joint between fully prefabricated pre-stressed concrete beam and high-strength reinforcement-confined concrete column, in order to further provide theoretical basis for the practical application.

2. Experimental design

2.1 Specimen design and construction fabrication

A total of 7 specimens are produced for the test. Among them, one specimen is the cross-shaped intermediate joint RC-01 for cast-in-place concrete, and the remaining six specimens are prefabricated cross-shaped intermediate joint, with beam cross-sections in the form of H-Section, among which the specimens PAN -03, PAN-04, PAN-05, and PAN-06 are used with dense spiral stirrup in the beam-end plastic hinge zone to confine the beam end concrete, to avoid compression on the beam end under the effect of the low cycle repeated load test that the concrete is collapsed and broken off, and the load-carrying capacity of the specimen is impaired. Specimen of reinforcement are shown in Table 1.

Table 1 Arrangement of reinforcement of specimen

<table>
<tr><th>Specimen</th><th>Strength of concrete</th><th>Cross section</th><th>Size (mm)</th><th>Longitudinal reinforcement</th><th>Stirrup spacing (mm)</th><th>Stirrup encryption area (mm)</th></tr>
<tr><td>Beam</td><td>C60</td><td>rectangle</td><td>400×400</td><td>16 ϕ 22 HRB600</td><td>50</td><td>30</td></tr>
<tr><td>RC-01</td><td>C60</td><td>rectangle</td><td>450×380</td><td>12 ϕ 22 HRB600</td><td>50</td><td>30</td></tr>
<tr><td>PAN-03</td><td>C40</td><td>I-shaped</td><td rowspan="6">h = 450
b_f = 380
b = 110
h_f = 150</td><td rowspan="6">4 ϕ 25 HTH1080
8 ϕ 18 HRB400</td><td>50</td><td>30</td></tr>
<tr><td>PAN-04</td><td>C40</td><td>I-shaped</td><td>50</td><td>30</td></tr>
<tr><td>PAN-05</td><td>C40</td><td>I-shaped</td><td>50</td><td>30</td></tr>
<tr><td>PAN-06</td><td>C40</td><td>I-shaped</td><td>50</td><td>30</td></tr>
<tr><td>PAN-07</td><td>C40</td><td>I-shaped</td><td>50</td><td>30</td></tr>
<tr><td>PAN-08</td><td>C40</td><td>I-shaped</td><td>50</td><td>30</td></tr>
</table>

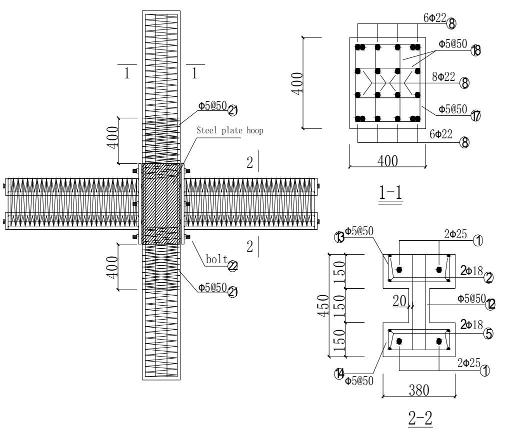

(a) Size and reinforcement of PAN-03~06 specimens

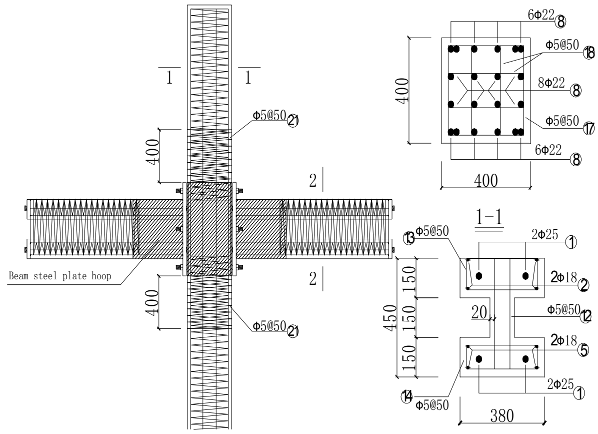

(b) Size and reinforcement of PAN-07~08 specimen

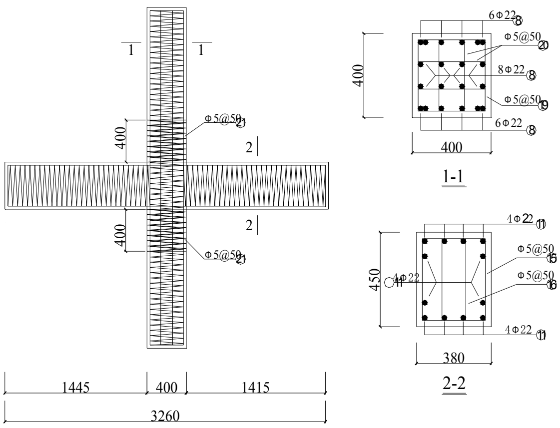

(c) Size and reinforcement of RC-01 specimens

Fig. 1 Size and Reinforcement of Specimen (Unit: mm)

Specimens PAN-07 and PAN-08 are installed with 4mm thick H-section steel plate stirrups in the range of 450 mm from the column edge to ensure that it will not fall off after the concrete develops into the plastic stage, and when the specimen reaches the ultimate load-carrying capacity, into the full ductility mode.

The core zones of the column joint are externally wrapped with 4mm thick steel plate stirrup, to prevent slippage of the welded dowel inside the steel plates. The beam-column stirrups are high-strength continuous compound spiral stirrup, with a yield strength of not less than 1100 MPa, stirrup in diameter of 5 mm, stirrup spacing of 30 mm in the dense zone and 50 mm in the non-dense zone. The end plate is used with Q390 grade 32 mm thick steel plate of good weld-ability and high-strength low-alloy structural steel to ensure that the beam longitudinal stress bars have clear path of force transfer. The upper and lower flanges of the beam are respectively arranged with 2 passes of pre-stressing bars, with yield strength of not less than 970 MPa, and a diameter of 25 mm. The specimen beam - columns have symmetrical reinforcement configuration, of which

Table 2 Mechanical properties of concrete

Specimen	Cube compressive strength f_{cu}/MPa	Axial compressive strength f_c /MPa	Modulus of elasticity E_c /MPa
Column	41.9	20.0	3.3×10^4
Beam	27.5	13.1	2.9×10^4

Table 3 Mechanical properties index of steel

Diameter or thickness	Yield strength f_y /MPa	Ultimate strength f_u /MPa	Modulus of elasticity E_s /MPa	Elongation rate after fracture, %	Strength-yield ratio
5	1157.51	1776.7	2.00×10^5	1.2	1.53
18	451.7	688.3	2.10×10^5	23.5	1.52
22	698.3	878.3	2.11×10^5	21	1.24
25	1026.67	1161.2	2.06×10^5	17	1.13
—4	296.7	448.3	2.03×10^5	29	1.51
—10	367.5	532.5	2.07×10^5	31.3	1.45

Table 4 Properties high strength grouting material

G-1 high-strength grouting material	Flexural strength /MPa	Compressive strength /MPa
	3.02	41.00

the design axial compression ratio of column is 0.27. The geometry and reinforcement of the specimen are as shown in Fig. 1.

2.2 Material properties

The mechanical properties of concrete materials (Zhao *et al*. 2012) are listed in Table 2. The reinforcement material indexes (Zhang *et al*. 2013) are as shown in Table 3. When pouring concrete specimen, reserved two groups of block size is 150 mm×150 mm×150 mm concrete cube and two groups of 150 mm×150 mm×300 mm concrete prism block. Test after, testing the cube and prism compressive strength of the block, and the tensile strength of steel.

When producing specimens, the G-1 high-strength grouts are used to pour densely the gaps generated during assembling of the beam - column joint, to achieve an adequate force transfer path. The flexural strength and compressive strength of high-strength grout material are shown in Table 4.

2.3 Pre-stressing force techniques

Post-tensioned application technology is used in this test. The pre-stressing tendons are single reinforcing steel bars that is anchored with high-strength nuts. The pre-stressing force is applied with 2000 N·m torque wrench. During the application of pre-stressing force, the strength of concrete in components shall meet the design requirements or can meet the strength standard value of 75%. The tensioning shall be carried out symmetrically, and multi-stage loading shall be

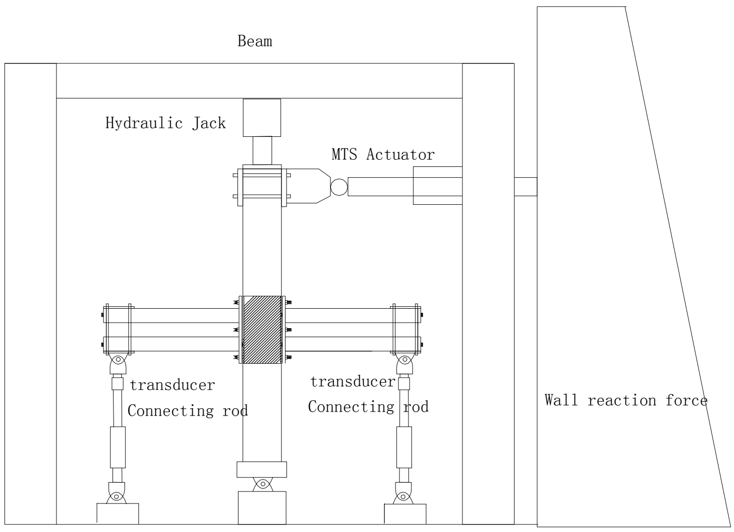

Fig. 2 Schematic view of the loading device

applied when the tensioning force is relatively greater. The pre-stressed tensioning procedures for this test are in sequence as: (a)pouring concrete structures or components (opening reserved) → (b) curing and formwork stripping → (c) measuring torque coefficient → (d) threading tendon and tensioning at one end (after attaining 75% of the strength) → (e) anchoring of nut → (f) moving and lifting.

2.4 Test equipment and loading system

The schematic views of the loading device are shown in Fig. 2. The beam - column joint specimens are used with column end loading method, the loading system is used with the force-displacement hybrid control loading method. According to the Specification of Test Methods for Earthquake Resistant Building (GBJ101-96) (Code for Design of Concrete Structures 2010), in the elastic stage, the stage-by-stage single reciprocating cyclic loading shall be applied with control by force and with stage differential of 30 kN. When the longitudinal ordinary rebar on the specimen beam end reaches the yield stage, the load shall be controlled by yield displacement multiples as the stage difference of loading. Each stage has a load repeat of 3 cycles, until the specimen fails or the load-carrying capacity of the specimen drops to about 85% of the ultimate load.

3. Test process and main failure characteristics (Li and Kai 2011)

The specimens for the pre-fabricated pre-stressed beam-column joints of PAN-03, PAN-04, PAN-05, PAN-06 are of the same conditions with the cross-section of the beam-column, the shear-span ratio of beam, the forms of reinforcement and the loading scheme, showing substantially similar characteristics of failure. At the early loading stage, the loads applied are small, and the specimens show no significant appearance changes. With the increase of load, the upper and lower flanges of the beam appear nearly vertical curved cracks firstly. Due to the constraints of pre-stressed reinforcement, the cracking load increases, the crack distribution states are basically the

(a) PAN-04 ultimate failure diagram

(b) PAN-08 ultimate failure diagram

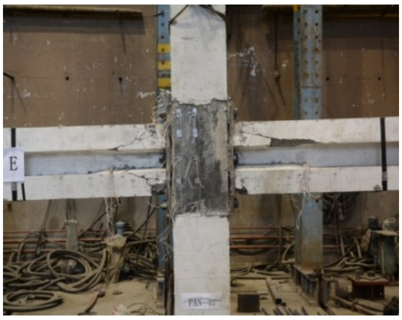

(c) PAN-03 ultimate failure diagram

(d) PAN-05 ultimate failure diagram

(e) PAN-06 ultimate failure diagram

(f) PAN-07 ultimate failure diagram

(g) RC-01 ultimate failure diagram

Fig. 3 Specimens ultimate failure modes

same, the web with certain distance from the column edge produces slight diagonal crack approximately in an angle of 30° with the beam axis. During the failure stage, the concrete on the beam end in the joint zone is crushed, the concrete cover of the beam end web spall off, and the beam end plates are slightly warped.

The load-carrying capacity and ductility of the specimens PAN-07 and PAN-08 for steel plate stirrup joint installed on the beam ends are basically the same as other prefabricated specimens. The concrete in the core zone of the joint is in a three-dimensional stress state under the simultaneous action of the steel plate stirrup and the end plate high-strength bolts, where no failure occurs, and the steel plate stirrups are intact in shape and free of any warping. The columns appear slight lateral tension crack in the loading process, and the crack is closed after the end of the test and it is, basically free of damage.

The listed ultimate failure modes of typical specimens are shown in Fig. 3. The Fig. 3 shows that prefabricated joint damage, occur in the beam end, and cast-in-place type joint failure happened in the joint core. So compared with cast-in-place joints, prefabricated joint intensity is higher, more reliable connection.

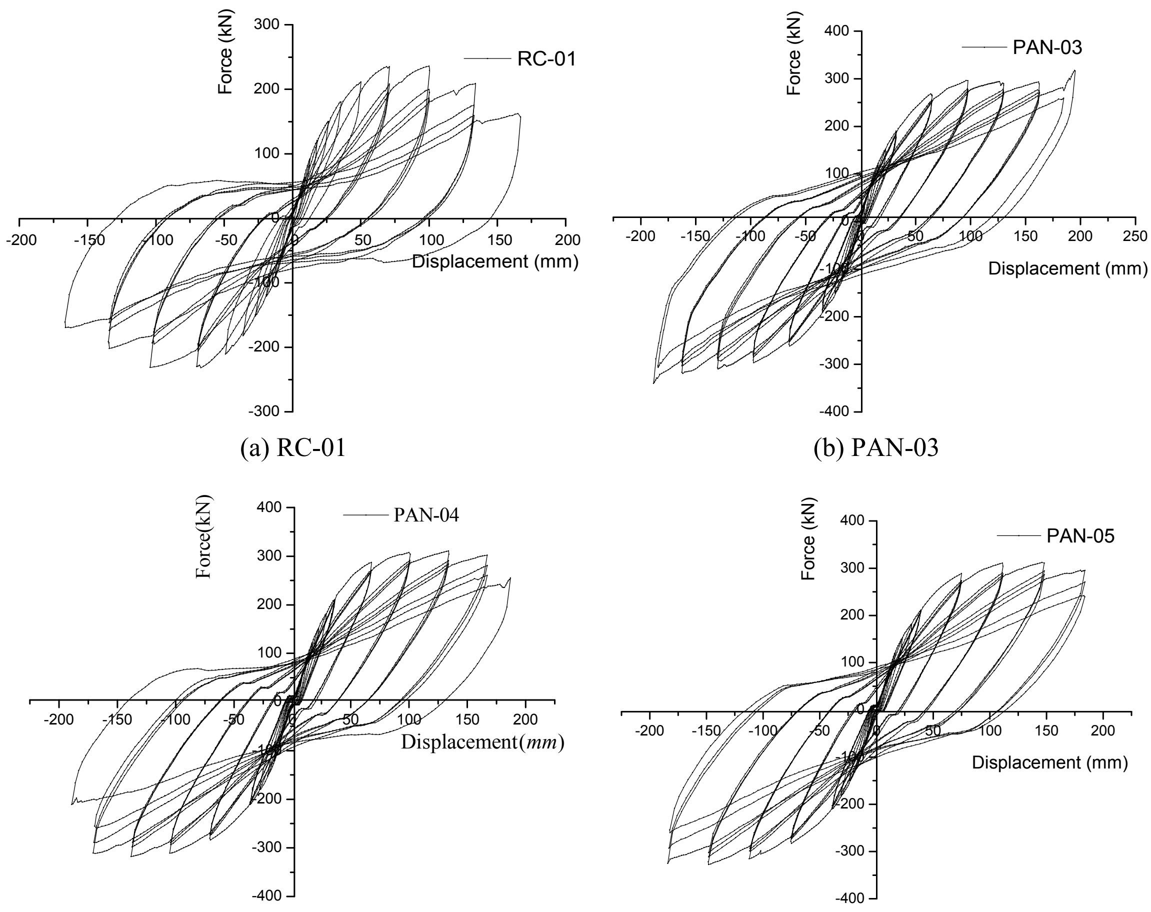

(a) RC-01

(b) PAN-03

(c) PAN-04

(d) PAN-05

Fig. 4 $P - \Delta$ curve of specimens

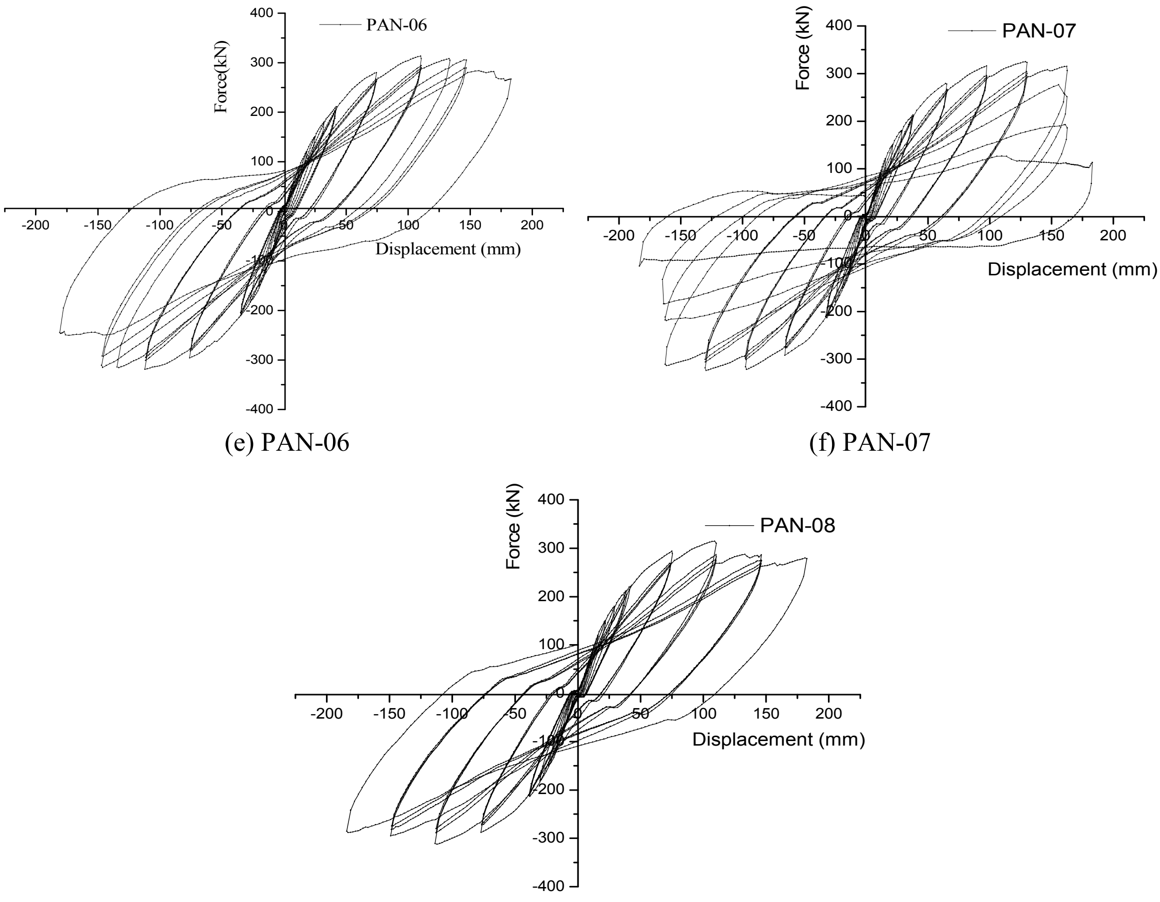

(e) PAN-06 (f) PAN-07

(g) PAN-08

Fig. 4 Coninued

4. Analysis on test results (Fu 2011, Tsonos 2008)

4.1 Hysteresis curve

Hysteresis curves, represented by column top horizontal load P and column top horizontal displacement Δ are studied in this paper. They are shown in Fig. 4. In general, the hysteresis curves are similar in shape, size and evolution process.

The joints of pre-fabricated pre-stressed concrete frames also exhibit certain characteristics of pure steel frame joints and reinforced concrete frame joints, as shown from Fig. 4, the hysteresis curves for early loading are in elongated fusiform. When the beam end longitudinal plain reinforcement yields, the hysteresis curve of the specimen is plump and spindle-shaped. When approaching failure, the load-carrying capacity of the specimen shows insignificant decrease after reaching the peak load, indicating that the internal core concrete on the beam end has higher load-carrying capacity under constraint of the high strength dense stirrups.

Compared with ordinary reinforced concrete structures, the hysteretic loop of joints in the precast pre-stressed prefabricated concrete framework is relatively long and narrow and has relatively small energy dissipation capacity. Through comparison of each level of equidirectional loading cycles, the slope of hysteretic curve for later control displacement is smaller than that of hysteretic curve for the former control displacement. This indicates that under cyclic load, the structural stiffness degrades with increase of horizontal displacement. Under the effect of the same level of control displacement, the structure has good resilience properties due to the presence of pre-stressing force, so that the unloading curves for three cycles converge, the stiffness barely degrades and the load-carrying capacity degradation is not obvious.

4.2 Skeleton curve (*Hossain and Ashraf 2012*)

The skeleton curves for each joint specimen in the precast pre-stressed assembly concrete frame are as shown in Fig. 5.

As can be seen from Fig. 5, the load increases linearly with the displacement before yield of specimen. After the specimens are cracked, the specimen stiffness decreases; when the specimen reaches peak load, the skeleton curve is close to horizontal, and the displacement increases substantially, but the loads basically no more increases, indicating that in this stage, the concrete on the beam end cracks, and most of the energies are consumed; continue loading until failure, the load-carrying capacity of the specimen decreases with increase in displacement. The change law of the skeleton curve for prefabricated pre-stressed concrete frame joints is basically the same as that cast-in-place reference specimens.

4.3 Ductility factor (*AISC 2005*)

The displacement ductility factor is used in the test, and the ratio μ of capital horizontal limit displacement and yield displacement is used to represent the component ductility. In order to accurately assess the displacement ductility factor of the prefabricated pre-stressed concrete girder-column joints, the most commonly used equivalent energy method is used in this paper to determine the yield displacement Δy of joint specimens. The principles for equivalent energy

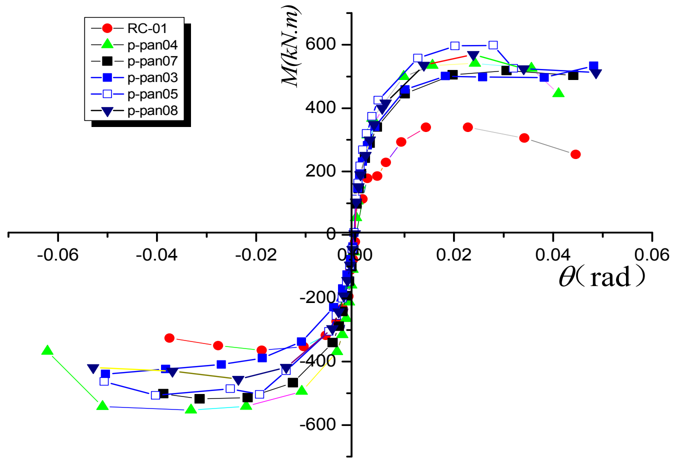

Fig. 5 Skeleton Curve of Specimens

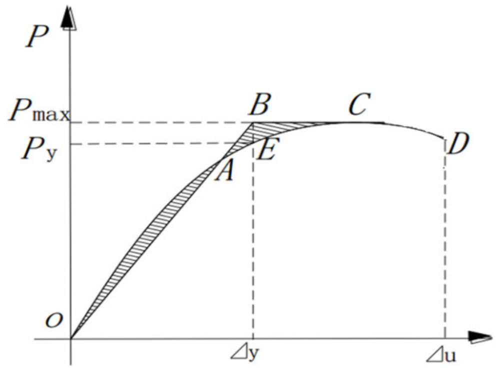

Fig. 6 Diagram of determination of specimen yield displacement by means of equivalent energy method

Table 5 Load characteristic values and displacement ductility of specimens

Specimen No.		Cracking load, P_c /kN	Yield load P_y /kN	Yield displacement, Δ_y /mm	Limit load P_u /kN	Ultimate displacement Δ_u /mm	Ductility factor μ
RC-01	Back	120	193.07	36.26	-227.02	132.91	3.67
	Front	90	194.51	38.39	232.22	134.07	3.49
PAN-03	Back	120	269.23	72.36	-316.78	186.14	2.57
	Front	120	247.87	53.4	294.98	193.2	3.62
PAN-04	Back	120	267.24	54.96	-316.52	168.42	3.06
	Front	120	262.4	52.44	309.79	176.99	3.38
PAN-05	Back	120	271.89	62.22	-319.01	163.54	2.63
	Front	120	259.25	52.13	310.05	163.54	3.14
PAN-06	Back	120	271.8	81.77	-318.91	172.31	2.11
	Front	120	277.87	79.87	319.74	177.66	2.22
PAN-07	Back	150	269.22	54.26	-320.67	159.3	2.94
	Front	150	272.81	59.25	321.35	160.15	2.70
PAN-08	Back	150	256.02	55.44	-307.61	176.25	3.18
	Front	150	257.09	55.04	309.23	152.53	2.77

method are shown in Fig. 6. Δu is the corresponding displacement values when the load drops to 85% of the maximum load. In this test, the load values for individual specimens have not dropped to the specified value due to the limited load displacement of test equipment. In this case, Δu is taken as the maximum loading displacement of equipment. The yield displacement, yield load, limit displacement, limit load and ductility factor of each specimen are shown in Table 5.

As can be seen from Table 4, the ductility factors (Zenunović and Folić 2012, Ma and Su 2010) on the cast-in-place reinforced concrete frame joints obtained in the previous tests are about 2.0~5.5, and the ductility coefficients on prefabricated specimen in this test are in such range, indicating that the joint has good deformability. The concrete in the core zone of joint for the cast-in-place specimen has oblique shear cracks, but the concrete in the core zone of joint does not exhibit brittleness under constraint of high-strength spiral stirrup, but can still take certain loads, reflecting the superiority of the high-strength stirrup.

4.4 Analysis on shear strength of joints (*Shayanfar et al. 2012*, *Panda et al. 2012*)

In order to achieve the effect of strong joint, the shear failure index of joint, J is introduced.

$$J = \frac{\sum a_t \sigma_y}{b_e D_b \alpha_1 \alpha_2 v \sigma_B}(1+\alpha) \tag{1}$$

$$\alpha_1 = 1 - \frac{0.1(\sigma_y - 350)}{350} \tag{2}$$

$$\alpha_2 = 1 - \frac{0.61 p_w \sigma_y}{\sigma_B} \tag{3}$$

$$\left.\begin{array}{ll} \alpha = 0 & \mu \le 3.2 \\ \alpha = \dfrac{(\mu - 3.2)}{3.2} & 3.2 < \mu \le 6.4 \\ \alpha = 1 & \mu > 6.4 \end{array}\right\} \tag{4}$$

$$v\sigma_B = 1.7\sigma_B^{2/3} \tag{5}$$

Where: $\sum a_t \sigma_y$ - the sum of the forces of the left and right beam joints;
a_t - Area of beam tension reinforcement;
σ_y - Yield strength of beam reinforcement;
b_e - Effective width of the beam-column joints, taking the average width of beam and column;
D_b - Section height of the beam;
$v\sigma_B$ - Effective concrete strength;
σ_B - Compressive strength of concrete;
p_w - Transverse reinforcement rate of the joint section parallel to the loading direction;
μ - Bond factor of joint.

$$\mu = \frac{2\tau_f}{\sqrt{\sigma_B}} = \left(\frac{d_b}{D_c}\right)\left(\frac{\sigma_y}{\sqrt{\sigma_B}}\right) \tag{6}$$

Where: D_c - the height of the column cross-section;
d_b - the diameter of the stressed reinforcement of the beam.

J < 1: Yield of beam before shear failure of joint; J = 1: Yield of beam at the time of shear failure of joint; J > 1: shear failure of the beam-column joints prior to yield of beam. The shear strength index of RC-01 joints can be calculated as: J = 1.36, greater than 1; indicating shear failure of the beam-column joints prior to yield of beam; while the shear strength index of PAN member joints: J = 1.851, less than 1, indicating the yield of beam before shear failure of joint.

The tests also confirmed this as shown in the following Fig. 7.

(a) RC-01 joint failure

(b) PAN joint failure

Fig. 7 Joint Failure

4.5 Stiffness degradation

With the constant increase in load-displacement, the cumulative damage of the specimens will cause degradation of stiffness with the increase in displacement (Fu 2011). The secant stiffness degradation curve of the specimen is as shown in Fig. 8.

As can be seen from Fig. 8:

(1) The stiffness of cast-in-place specimen is slightly smaller than that of the prefabricated specimen, probably due to the occurrence of shear failure of concrete in the core zone of joint of the cast-in-place specimens during loading, the load-carrying capacity slightly lower than that of the prefabricated specimen, the stiffness degradation is obvious and the energy dissipation capacity is weak.

(2) The stiffness degradation trends of the prefabricated specimens are roughly the same. When entering the yield stage, the stiffness degradation is obvious. The main reason may be that during early loading of prefabricated specimen, the specimen exhibits good integrity and great stiffness due to the effect of initial pre-stressing force of high-strength

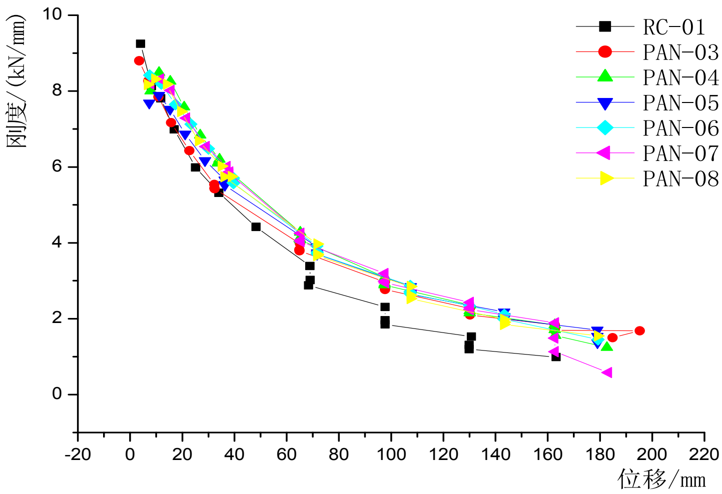

Fig. 8 Specimen Stiffness Degradation Curve

bolts; with the development of displacement, the beam end moment increases correspondingly, the beam end longitudinal reinforcement reaches the yield, and the cracks in the plastic hinge zone of the beam end grow more and wider. At the same time, the cumulative damage of the specimen and the bond-slip between steel and concrete make the stiffness of specimen decrease.

(3) During late loading of the specimen, with the increase in displacement, the stiffness degradation rate becomes slow. The main reason is possibly because the concrete cracks have fully developed during late loading, and no new crack appears. Under repeated loading, the tension cracks in the plastic hinge zone on the end of the beam only open in closure state, so that the influence on the stiffness degradation is not obvious.

5. Conclusions

Through the low cycle repeated loading tests on the specimens of the end plate bolt connecting joint between fully prefabricated pre-stressed concrete beam and high-strength reinforcement-confined concrete column, the following conclusions can be drawn:

(1) Under action of the horizontal repeated loading, the hysteresis curves of specimens develop symmetrically. Under action of pushing and tension repeated loading, the lateral stiffness and load load-carrying capacity of specimens are substantially the same, and the specimen has good seismic performance. The number of cycles has little effect on the load-carrying capacity degradation of the joints.

(2) The stiffness degradation trends of the specimens are substantially the same. During later period of loading of the specimen, the stiffness degradation becomes slow, the stiffness of the cast-in-place specimens is slightly less than that of the prefabricated specimen.

(3) The ductility factors of the cast-in-place reinforced concrete frame joints are 2.0~5.5, while the ductility factors of the joints of the prefabricated specimens are within the range, indicating that the joint has better deformability.

(4) The prefabricated beam-column can meet the requirements for strong joint and weak member in some extent, and the prefabricated joint has good resistance to shear.

References

AISC (2005), Seismic provision for structural steel building, American Institute of Steel Structure.

Ban, S.L. (2011), "Experimental studies on dimensional effect on characteristics of stirrups confined concrete", Dalian University of Technology, Dalian, China.

Fu, J.F. (2011), "Experimental studies on stress characteristics of construction waste recycled aggregate concrete and component", Zhengzhou University, Zhengzhou, China.

GB 2010 (2010), Code for Design of Concrete Structures.

Ho, I.F.Y., Lam, E.S.S., Wu, B. and Wang, Y.Y. (2013), "Monotonic behavior of reinforced concrete columns confined with high-performance ferrocement", *J. Struct. Eng. – ASCE*, **139**(4), 574-583.

Hossain, M.R. and Ashraf, M. (2012), "Mathematical modelling of yielding shear panel device", *Thin-Wall. Struct.*, **59**, 153-161.

Hossain, M.R., Ashraf, M. and Albermani, F. (2011), "Numerical modelling of yielding shearpanel device for passive energy dissipation", *Thin-Wall. Struct.*, **49**(8), 1032-1044.

Hou, W.L. (2011), "Performance test and theoretical study on joint between square pipe concrete special-shaped column and steel beams", Xi'an University of Architecture and Technology, Xi'an, China.

Jian, B., Zhong, Q., Gan, Y. and Wang, Y.P. (2013), "Experimental studies on low-frequency cyclic load on transfer structure for prestressed concrete empty web truss", *China Civil Eng. J.*, **46**(12), 18-24.

Karayannis, C.G. and Sirkelis, G.M. (2008), "Strengthening and rehabilitation of RC beam–column joints using carbon-FRP jacketing and epoxy resin injection", *Earthq. Eng. Struct. D*, **37**(5), 769-790.

Le-Trung, K., Lee, K., Lee, J., Lee, D.H. and Woo, S. (2010), "Experimental study of RC beam–column joints strengthened using CFRP composites", *Compos. Part B – Eng.*, **41**(1), 76-85.

Li, B. and Kai, Q. (2011), "Seismic behavior of reinforced concrete interior beam-wide columnjoints repaired using FRP", *J. Compos. Constr.*, **15**(3), 327-338.

Liang, X.W., Xin, L., Deng, M.K., Fang, L. and Zhang, X.H. (2010), "Experimental studies on seismic behavior and performance indicators of high-strength concrete shear wall", *China Civil Eng. J.*, **11**, 37-45.

Liu, L. (2011), "Eberimental study on uni-axial compression constitutive relation of corroded stirrup confined concrete", Xi'an University of Architecture and Technology, Xi'an, China.

Liu, Z.Q., Xue, J.Y., Ni, M.M., Zhao, P. and Zhao, H.T. (2012), "Quasi-static test and finite element force analysis on solid web shaped reinforced concrete columns side frame", *J. Build. Struct.*, **33**(8), 23-30.

Ma, G.Y. and Su, Y.P. (2010), "Calculation formulas for ultimate compressive strength and strain of FRP confined concrete cylinder", *J. Hebei Univ. Sci. Technol.* (Natural Science Edition), **1**, 74-77.

Mu, X.T., Jian, S.F. and Jian, G.N. (2013), "Seismic behavior of steel reinforced concrete column–steel truss beam hybrid joints", **56**, 1557-1569.

Niroomandi, A., Maheri, A., Maheri, M.R. and Mahini, S.S. (2010), "Seismic performance of ordinary RC frames retrofitted at joints by FRP sheets", *Eng. Struct.*, **32**(8), 2326-2336.

Panda, K.C., Bhattacharyya, S.K. and Barai, S.V. (2012), "Shear behaviour of RC T-Beams strengthened with U-wrapped GFRP sheet", *Steel Compos. Struct., Int. J.*, **12**(2), 149-166.

Pantelides, C.P., Okahashi, Y. and Reaveley, L.D. (2008), "Seismic rehabilitation of reinforced concrete frame interior beam–column joints with FRP composites", *J. Compos. Constr.*, **12**(4), 435-445.

Rao, G.A. and Sundaresan, R. (2012), "Evaluation of size effect on shear strength of reinforced concrete deep beams using refined strut-and-tie model", *Sadhana*, **37**(1), 89-105.

Sasmal, S., Novak, B., Rmanjaneyulu, K., Roehm, C., Srinivas, V. and Lakshmanan, N. (2011), "Upgradation of gravity load designed sub-assemblages subjected to seismic type loading", *Compos. Struct.*, **93**(6), 1561-1573.

Shayanfar, M.A., Barkhordari, M.A. and Rezaeian, A.R. (2012), "Experimental study of cyclic behavior of composite vertical shear link in eccentrically braced frames", *Steel Compos. Struct., Int. J.*, **12**(1), 13-29.

Shi, Q.X., Wang, N., Tian, Y., Wang, P. and Li, K. (2013), "Studies on axial compression stress - strain full curve for high-strength stirrups confined high-strength concrete", *J. Build. Struct.*, **34**(4), 144-151.

Tsonos, A.G. (2008), "Effectiveness of CFRP-jackets and RC-jackets in post-earthquake and pre-earthquake retrofitting of beam–column subassemblages", *Eng. Struct.*, **30**(3), 777-793.

Xu, M., Peng, Z. and Chen, Z.F. (2013), "Experimental study on seismic behavior of load-bearing walls with insulation concrete compound block masonry of new-type concrete", *Industrial Construction Magazine Agency*, **43**(3).

Yao, R. (2010), "Studies on seismic behaviors of precast prestressed fabricated beam-column joints", Beijing University of Civil Engineering and Architecture, Beijing, China.

Zenunović, D. and Folić, R. (2012), "Models for behaviour analysis of monolithic wall and precast or monolithic floor slab connections", *Eng. Struct.*, **40**, 466-478.

Zhang, Z.C. (2013), "Studies on seismic behavior of concrete columns confined by plate bolt tendon connected high strength stirrups", Xi'an University of Architecture and Technology, Xi'an, China.

Zhang, Q., Jiang, Q. and Lu, X.Z. (2013), "Studies on influences of lateral impact on compressive bearing capacities of steel pipe concrete", *Struct. Eng.*, **29**(3), 59-64.

Zhao, B.C, Zhu, H., He, R.Q. and Gu, Q. (2012), "Experimental study on through-bolt-end-plate connecting joint between steel pipe concrete columns and trusses", Xi'an University of Architecture and Technology (Natural Science Edition), **44**(2), 170-176.

CC